Generalization of Space-Time Block Coded-Spatial Modulation for High Data Rate VLC Systems

(Invited Paper)

Shimaa A. Naser
Khalifa University
Abu Dhabi, 127 788, UAE
e-mail: shimaa.naser@ku.ac.ae

Paschalis C. Sofotasios
Khalifa University, Abu Dhabi, 127 788, UAE
Tampere University, Tampere, 33101, Finland
e-mail: p.sofotasios@ieee.org

***Abstract*—Visible light communication (VLC) is a promising solution to the current congestion in radio frequency (RF) spectrum. It achieves that by exploiting the huge unregulated visible light portion of the electromagnetic spectrum in order to enable high-speed short range wireless communications, as well as, providing an sufficient lighting. This new solution is envisioned to provide a considerably wider bandwidth that can accommodate ubiquitous broadband connectivity to indoor users and further offload data traffic from overloaded cellular networks. However, VLC suffers from several limitations, such as the limited modulation bandwidth of light-emitting diodes (LEDs) that degrades the overall system spectral efficiency. In this respect, several interesting solutions have been proposed in the recent literature to overcome this limitation, such as the implementation of efficient optical modulation and multiple-input-multiple-output (MIMO) schemes. In this paper, we investigate the performance of multiple active spatial modulation (MASM) integrated with orthogonal space time block codes (STBC) for indoor VLC systems. Additionally, in ordered to reduce the receiver complexity, a simplified version of the joint maximum likelihood (ML) detector is proposed which has a linear complexity with respect to the number of transmit LEDs and the constellation size. Extensive computer simulations demonstrate that STBC-MASM improves the overall system performance compared to MASM with a considerably simplified detection.**

***Index Terms*—GSSK, MIMO, MASM, STBC, visible light communication.**

I. INTRODUCTION

VIsible light communication (VLC) has emerged as a promising alternative to the current congested RF spectrum aiming to provide Gbps data rates to mobile users. The key principle of VLC technology is to utilize the emitted light from the light emitting diodes (LEDs) in the ceiling to perform data transmission through intensity modulation and direct detection (IM/DD), without affecting their main illumination function. Also, VLC systems exhibit other advantages including security, high degree of spatial reuse, and immunity to electromagnetic interference (EMI) [1]. Yet, despite the aforementioned advantages of VLC systems, several key factors affect negatively the overall system performance. These are the limited modulation bandwidth and the peak optical power of LEDs and are considered as the main constraints towards realizing the full potential of VLC systems [2]. Therefore, several analyses have been carried out attempting to enhance the spectral efficiency of VLC systems through the development of different optical-based modulation and coding schemes, adaptive modulation, equalization, VLC cooperative communications, multiple access, and multiple-input-multiple-output (MIMO) schemes.

It is recalled that MIMO transmission techniques have been comprehensively studied in the context of RF communications and they have showed an improvement in terms of system capacity and reliability compared to conventional single-input-single- output (SISO) systems. In general, two strategies were developed in the literature namely, space time block codes (STBC) and spatial multiplexing (SMP). It is recalled that SMP schemes provide an enhancement on the achievable data rate by transmitting multiple data streams from multiple LEDs. However, the incurred inter-channel interference (ICI) and the involved decoding complexity are the two major drawbacks that limit its performance [3]–[5]. On the other hand, orthogonal STBCs offer different features such as, allowing reliable communication and reduced implementation and decoding complexity [6]. In the same context, researchers have recently investigated extensively the newly emerged index modulation (IM) techniques because of their promising high spectral efficiency [7], [8]. The fact that IM relies on the activation of one of the building blocks of the communication system such as the transmitting LED, frequency, time slot, or combination of them allows the transmission of more information. Likewise, space shift keying (SSK), generalized space shift keying (GSSK), and spatial modulation (SM) are all forms of IM in which the indices of the LEDs are used to convey extra information [9]–[11]. Yet, it is noted that they are all limited in terms the number of required LEDs to achieve higher spectral efficiency.

Multiple active spatial modulation (MASM) is a generalized version of SM that highly enhances the spectral efficiency by

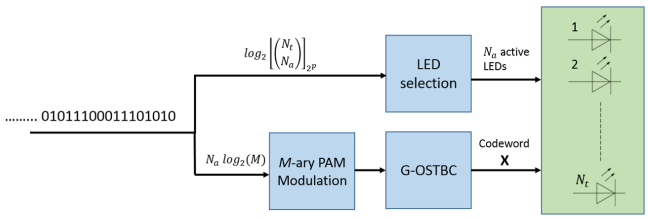

Fig. 1. Generalized STBC-MASM transmitter

conveying more information in both spatial and signal domains [12]–[14]. MASM relies on the activation of N_a LEDs out of N_t simultaneously based on spatial bits. Moreover, a distinct real non-negative M-ary symbols are transmitted from each active LED. It was shown in [15] that MASM achieves high spectral efficiency but, one of its major drawbacks is the degraded bit error rate (BER) performance particularly when the number of the activated LEDs increases as well as, when higher M-ary modulation size is used. Combining STBC with SM has achieved significant performance improvement over SM in RF systems by exploiting the advantages of both SM and STBC without any increment in the transmitted power [16], [17]. However, in the context of VLC systems, STBC-SM has not been investigated so far. With this motivation, the aim of this paper is to study the benefits of combining orthogonal STBC with MASM in VLC systems. To the best of the authors knowledge, the offered results are novel and have not been reported before in the open technical literature.

The remainder of this paper is organized as follows: In section II, we present the basic system and channel models. Generalization of Alamouti STBC for VLC systems for any number of active LEDs, N_a, and any M-ary PAM modulation size is introduced in section III, whereas Section IV introduces a simplified ML detection. In Section V we present the corresponding simulation results for the STBC-MASM and MASM techniques. Finally, Section VI summarizes and concludes the paper.

Notations: In what follows, boldface uppercase and lowercase represent matrices and vectors, respectively. $(\cdot)^T$ denotes the transpose operation, $|\cdot|$ is the absolute value operation, $\boldsymbol{I}$ is the identity matrix, $\binom{N}{k}$ is the binomial coefficient, $\lfloor x \rfloor$ is the largest integer less than or equal x, $\lfloor x \rfloor_{2^p}$ is the largest integer less than or equal x, that is integer power of 2, and $\mathcal{N}(0,\sigma^2)$ is a real-value Gaussian distribution with zero mean and variance σ^2.

II. System and Channel Models

We consider an indoor downlink VLC multiple-input-single-output (MISO) system employing IM/DD of the optical carrier using LEDs. The room size is $5 \times 5 \times 4\ m^3$ and is equipped with N_t transmit LEDs and a single photo detector (PD) receiver. Fig. 1 illustrates the basic system model of STBC-MASM. The coming bit stream is divided into two parts: the first $\log_2(\lfloor\binom{N_t}{N_a}\rfloor_{2^p})$ are used to select the indices of the LEDs that will be activated, with N_a denoting the number of active LEDs. Moreover, the other $N_a \log_2(M)$ bits are initially modulated through M-ary pulse amplitude modulation (PAM) then, encoded using an orthogonal STBC to generate a codeword $\mathbf{X}$ that is transmitted through the active LEDs. Based on this, the received signal of the STBC-MASM system is expressed as

$$\mathbf{y} = \frac{\eta}{N_a}\mathbf{X}\,\mathbf{h} + \mathbf{n}, \tag{1}$$

where, η is the PD responsivity and $\mathbf{X}$ is the transmitted codeword. Moreover, $\mathbf{n}$ is an additive white Gaussian noise (AWGN) with zero mean and variance $\sigma^2 = \sigma^2_{shot} + \sigma^2_{th}$, which is the sum of ambient light shot noise and thermal noise, respectively[1]. Finally, $\mathbf{h}$ is the DC channel gain vector from the active LEDs to the PD, which is considered only due to the line of sight (LoS) and each component can be expressed as follows: [19]

$$h_i = \begin{cases} \frac{A}{d_i^2} R_o(\varphi_i) T_s(\phi_i) g(\phi_i) \cos(\phi_i), & 0 \leqslant \phi_i \leqslant \phi_c \\ 0, & \text{otherwise}, \end{cases} \tag{2}$$

where A denotes the PD area, d_i is the distance between the i^{th} LED and PD, φ_i is the angle of transmission from the i^{th} LED to the PD, ϕ_i is the incident angle with respect to the receiver, and ϕ_c is the field of view (FoV) of the PD. Moreover, $T_s(\phi_i)$ is the gain of the optical filter and $g(\phi_i)$ is the gain of the optical concentrator, expressed as

$$g(\phi_i) = \begin{cases} \frac{n^2}{\sin^2(\phi_c)}, & 0 \leqslant \phi_i \leqslant \phi_c \\ 0, & \phi_i > \phi_c, \end{cases} \tag{3}$$

where n is the refractive index, and $R_o(\varphi_i)$ is the Lambertian radiant intensity given by the following:

$$R_o(\varphi_i) = \frac{m+1}{2\pi}\left(\cos(\varphi_{k,i})\right)^m, \tag{4}$$

where m denotes the order of the Lambertian emission, which is expressed as

$$m = \frac{-\ln(2)}{\ln\left(\cos(\varphi_{1/2})\right)}, \tag{5}$$

where $\varphi_{1/2}$ denotes the LED semi-angle at half power.

In what follows, we provide a general procedure to produce any real orthogonal STBC with any M-ary PAM constellation size.

III. Generalized STBC for VLC systems

In this section, we first consider the generalization of Alamouti STBC to any M-ary PAM symbols. Then, we provide a general procedure to produce real STBC for any number of active LEDs, N_a. To this end, we start with the well-known Alamouti STBC for two active LEDs, namely

$$\mathbf{X}_2 = \begin{bmatrix} x_1 & x_2 \\ \bar{x_2} & x_1 \end{bmatrix} \tag{6}$$

[1]More details on the calculation of the noise variance are provided in [18].

where, x_1 and x_2 are real and positive PAM symbols. Moreover, $\bar{x_i}$ denotes the complement of x_i which is for the case of on-off keying (OOK) and is calculated as $\bar{x_i} = A - x_i$. Yet, for any M-ary PAM constellation size, the symbols are defined as follows

$$x_i \in \frac{2iI_p}{M+1}, \qquad i = 1, 2, ..., M. \tag{7}$$

where I_p is the average transmitted optical power. Based on the above, we defined the complement of the symbol x_i as follows

$$\bar{x_i} = -x_i + \frac{2I_p}{M+1} + \frac{2MI_p}{M+1}, \qquad i = 1, 2, ..., M. \tag{8}$$

Next, Alamouti STBC can be generalized to produce an $N_a \times N_a$ STBC of rate 1, which can be utilized to activate N_a LEDs, namely

$$\mathbf{X_{N_a}} = \left[\begin{array}{c|c} \mathbf{X}^1_{\frac{N_a}{2}} & \mathbf{X}^2_{\frac{N_a}{2}} \\ \hline (\mathbf{X}^2_{\frac{N_a}{2}})^T & \mathbf{X}^1_{\frac{N_a}{2}} \end{array}\right] \tag{9}$$

where $\mathbf{X}^1_{\frac{N_a}{2}}$ and $\mathbf{X}^2_{\frac{N_a}{2}}$ are the $(N_a/2 \times N_a/2)$ STBC matrices for the first $N_a/2$ and the last $N_a/2$ symbols, respectively. The process starts by dividing the $N_a \times N_a$ matrix into blocks of size $N_a/2 \times N_a/2$. Then, each block is also divided into new sub-blocks until the smallest sub-block (i.e Alamouti matrix) is reached. For the sake of illustration, we will consider the special case of 8×8 STBC matrix. First, we start with dividing the 8×8 STBC matrix into blocks of size 4×4 as follows:

$$\mathbf{X_8} = \left[\begin{array}{c|c} \mathbf{X}^1_4 & \mathbf{X}^2_4 \\ \hline (\mathbf{X}^2_4)^T & \mathbf{X}^1_4 \end{array}\right] \tag{10}$$

where $\mathbf{X}^1_4$ and $\mathbf{X}^2_4$ are 4×4 codewords for (x_1, x_2, x_3, x_4) and (x_5, x_6, x_7, x_8), respectively. After that, each block is divided into a smaller 2×2 STBC sub-blocks as follows

$$\mathbf{X^1_4} = \left[\begin{array}{c|c} \mathbf{X}^1_2 & \mathbf{X}^2_2 \\ \hline (\mathbf{X}^2_2)^T & \mathbf{X}^1_2 \end{array}\right], \mathbf{X^2_4} = \left[\begin{array}{c|c} \mathbf{X}^3_2 & \mathbf{X}^4_2 \\ \hline (\mathbf{X}^4_2)^T & \mathbf{X}^3_2 \end{array}\right] \tag{11}$$

where $\mathbf{X}^1_2$ and $\mathbf{X}^2_2$ are Alamouti STBC codewords for (x_1, x_2) and (x_3, x_4) , respectively. On the other hand, $\mathbf{X}^3_2$ and $\mathbf{X}^4_2$ are Alamouti STBC codewords for (x_5, x_6) and (x_7, x_8), respectively. Note that the generated codwords satisfy the orthogonality condition $\mathbf{X_i^T X_i} = \mathbf{I}$.

IV. Proposed Simple ML Decoding

In this section, we propose the design of a simplified version of the ML detector. Using the received vector $\mathbf{y}$ in equation (1), the joint ML detector would decide on the indices and signal domain symbols jointly after T time slots based on the minimum distance between the received vector $\mathbf{y}$ and all potential combinations, i.e.

$$[\hat{\ell}, \hat{\mathbf{X}}] = \arg \min_{\tilde{\ell} \in \ell, \tilde{X} \in \mathbb{X}} \left\| \mathbf{y} - \frac{\eta}{N_a} \tilde{\mathbf{X}} \mathbf{h}_{\tilde{\ell}} \right\|^2 \tag{12}$$

It is noted here that joint ML detection requires the search over all $M^{N_a} \times \lfloor \binom{N_t}{N_a} \rfloor_{2^p}$ combinations, which in turn increases the detector complexity. The orthogonal property of STBCs allows the symbols x_i's to be decoded independently. Which reduces the complexity to $M \times N_a \times \lfloor \binom{N_t}{N_a} \rfloor_{2^p}$. We also propose a detector that reduces the complexity furthermore to $M \ N_a + \lfloor \binom{N_t}{N_a} \rfloor_{2^p}$ by breaking-down the detection process into two stages. The first stage involves the detection of the indices by considering the conditional ML detection (blind receiver) and assuming equally probable symbols as follows:

$$\hat{\ell} = \arg \min_{\tilde{\ell} \in \ell} \left\| \min_{X \in \mathbb{X}} \left[\left(\mathbf{y} - \frac{\eta}{N_a} \mathbf{X} \mathbf{h}_{\tilde{\ell}} \right) | \mathbf{X} \right] \right\|^2. \tag{13}$$

To this effect and since the generated STBC are orthogonal, the received signal can be processed using the effective detected channel gain matrix (assuming that the indices are decoded correctly) to decouple the signal domain symbols, yielding

$$\mathbf{H^T_{\ell_{eff}}} \mathbf{y} = \check{\mathbf{y}} = \|\mathbf{h}_\ell\|^2 . \frac{\eta}{N_a} I. \ \mathbf{x} + \mathbf{z}, \tag{14}$$

where, $\mathbf{x}$ is the vector of the transmitted symbols, and $\mathbf{z}$ is an AWGN vector with each component having a zero mean and a variance of $\sigma^2 \|\mathbf{h}_\ell\|^2$. Finally, a conventional signal domain ML detector is utilized to decide on each transmitted symbol separately, namely

$$\hat{x_i} = \arg \min_{\tilde{x_i} \in \chi} \left| \check{y_i} - \|\mathbf{h}_\ell\|^2 . \frac{\eta}{N_a} \tilde{x_i} \right|^2. \tag{15}$$

To the best of the authors' knowledge, the offered results have not been previously reported in the open technical literature.

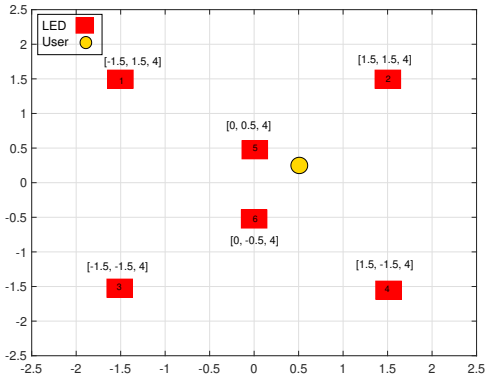

Fig. 2. LEDs and user placements in $5 \times 5 \times 4$ m^3 room.

V. Simulation

This section provides a thorough comparison of the performance of the STBC-MASM with that of MASM. To this end, we consider an indoor VLC environment where the room dimension is $5 \times 5 \times 4$ m^3. In addition, there are six transmit LEDs which are assumed to radiate perpendicularly from the ceiling to the floor. On the other hand, the receiver is located randomly on a desk at 0.8 m height from the floor and is assumed to be fixed throughout the simulations. The receiver is also assumed to be perpendicularly oriented from the desk to the ceiling. The positions of the transmit LEDs and the receiver are well illustrated in Fig. 2. The half-illuminance semi-angle of the LED is set to 60^o, which is a typical value for commercially-available high-brightness LEDs. For convenience, all the parameters involved in our simulations are summarized in Table.I.

A comparison between MASM and STBC-MASM systems in terms of the BER performance is considered in Fig. 3. It is evident that integrating STBC with MASM improves significantly the BER even for a single PD receiver and for large constellation size M. For instance at $M = 2$, more than 20 dB is required to achieve a BER of 10^{-3} using MASM compared to STBC-SM. Additionally, STBC-MASM user exhibits a good BER performance in the typical transmit SNR range for VLC system, where the received SNR in this case has an offset of 120 dB since the channel gain is in the

TABLE I
SIMULATION PARAMETERS.

Parameter	Symbol	Value
Room dimensions	-	$5 \times 5 \times 4m^3$
LED beam angle	$\varphi_{1/2}$	60^o
PD area	A	$1\ cm^2$
Refractive index of PD	n	1.5
Gain of optical filter	$T_s(\phi_i)$	1
FoV of PD	ϕ_c	60^o
PD responsivity	R	$1A/W$

order of 10^{-6}. Moreover, it can be seen that the derived bound on the BER for the proposed detector forms an upper bound that is very tight at high SNR values. For more fair comparison, we consider the BER performance for both schemes for a fixed spectral efficiency η of 4 and 5 bpcu, as depicted in Fig. 4. We observe that, STBC-MASM provides an enhancement on the system reliability compared to MASM in the typical SNR range for VLC systems. For instance, for $\eta = 4$ at transmit SNR=160 dB, the BER performance for STBC-MASM and MASM, is 10^{-4} and 10^{-3}, respectively.

Finally, a comparison in terms of the achievable throughput for both schemes is illustrated in Fig. 5. We observe that, in the typical SNR range, the throughput gap between the two schemes decreases as the constellation size increases, which is due to the high BER occurs in the case of MASM. Meanwhile, it is shown that using STBC codes improves the BER performance, which would reflects on the achievable data rate.

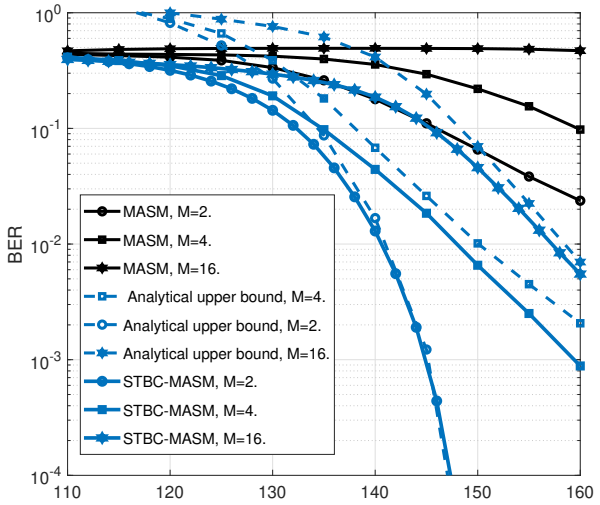

Fig. 3. BER performance comparison versus $N_t = 6$, $N_a = 2$, and $N_r = 1$ for transmit SNR.

VI. CONCLUSION

In this paper, we considered the performance of a high-rate low complexity MIMO transmission STBC-MASM scheme for VLC systems. Moreover, a general technique has been presented to construct any STBC-MASM scheme for any constellation size and any number of transmitting LEDs. It has been shown through out simulations that STBC-MASM is a promising MIMO technique for indoor VLC system that offers improved system BER performance and throughput compared to MASM. To achieve that, part of the bit stream was used to activate a group of the available LEDs, while the other part of the bit stream is conveyed through space time coded intensity modulation. Moreover, it has been shown through simulations that

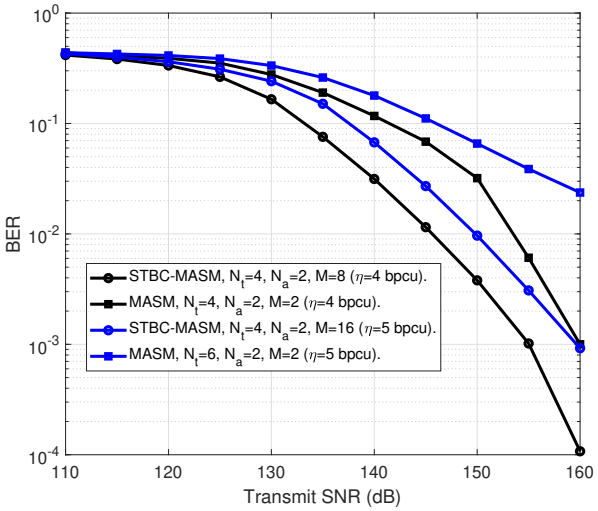

Fig. 4. BER performance comparison between STBC-MASM and MASM for spectral efficiencies of 4 and 5 bpcu. Black lines account for 4 bpcu and blue lines account for 5 bpcu.

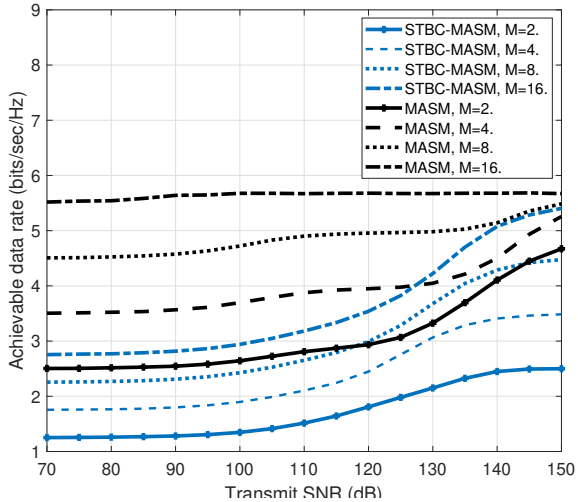

Fig. 5. Rate performance comparison between STBC-MASM and MASM for $N_t = 6$, $N_a = 2$, and $N_r = 1$ versus transmit SNR.

STBC-MASM maintains a good performance even in correlated channels and showed an improved throughput as the constellation size increases compared to MASM. The offered results are novel and provided meaningful insights that will be useful in the design and deployment of VLC systems.

ACKNOWLEDGMENT

This work was supported by Khalifa University under Grant KU/FSU-8474000122 and Grant KU/RC1-C2PS-T2/8474000137.

REFERENCES

[1] L. Grobe, A. Paraskevopoulos, J. Hilt, D. Schulz, F. Lassak, F. Hartlieb, C. Kottke, V. Jungnickel, and K. Langer, "High-speed visible light communication systems," *IEEE Commun. Mag.*, vol. 51, no. 12, pp. 60–66, Dec. 2013.

[2] A. Jovicic, J. Li, and T. Richardson, "Visible Light Communication: Opportunities, Challenges and The Path To Market," *IEEE Commun. Mag.*, vol. 51, no. 12, pp. 26–32, Dec. 2013.

[3] P. M. Butala, H. Elgala, and T. D. C. Little, "Performance of optical spatial modulation and spatial multiplexing with imaging receiver," in *2014 IEEE Wireless Communications and Networking Conference (WCNC)*, April 2014, pp. 394–399.

[4] P. W. Wolniansky, G. J. Foschini, G. D. Golden, and R. A. Valenzuela, "V-blast: an architecture for realizing very high data rates over the rich-scattering wireless channel," in *1998 URSI International Symposium on Signals, Systems, and Electronics. Conference Proceedings (Cat. No.98EX167)*, Oct 1998, pp. 295–300.

[5] S. M. Khan, N. Saha, M. R. Rahman, M. Hasan, and M. S. Rahman, "Performance improvement of mimo vlc using v-blast technique," in *2016 5th International Conference on Informatics, Electronics and Vision (ICIEV)*, May 2016, pp. 45–49.

[6] V. Tarokh, H. Jafarkhani, and A. R. Calderbank, "Space-time block codes from orthogonal designs," *IEEE Transactions on Information Theory*, vol. 45, no. 5, pp. 1456–1467, July 1999.

[7] X. Cheng, M. Zhang, M. Wen, and L. Yang, "Index modulation for 5g: Striving to do more with less," *IEEE Wireless Communications*, vol. 25, no. 2, pp. 126–132, April 2018.

[8] T. Mao, Q. Wang, Z. Wang, and S. Chen, "Novel index modulation techniques: A survey," *IEEE Communications Surveys Tutorials*, vol. 21, no. 1, pp. 315–348, Firstquarter 2019.

[9] T. Fath and H. Haas, "Performance comparison of mimo techniques for optical wireless communications in indoor environments," *IEEE Transactions on Communications*, vol. 61, no. 2, pp. 733–742, February 2013.

[10] C. R. Kumar and R. K. Jeyachitra, "Performance comparison of space shift keying mimo techniques for visible light communication," in *2017 International Conference on Intelligent Computing and Control (I2C2)*, June 2017, pp. 1–4.

[11] A. Stavridis and H. Haas, "Performance evaluation of space modulation techniques in vlc systems," in *2015 IEEE International Conference on Communication Workshop (ICCW)*, June 2015, pp. 1356–1361.

[12] C. Rajesh Kumar and R. K. Jeyachitra, "Power efficient generalized spatial modulation mimo for indoor visible light communications," *IEEE Photonics Technology Letters*, vol. 29, no. 11, pp. 921–924, June 2017.

[13] D. Li, W. Zhang, J. Sun, and C. Wang, "An improved generalized spatial modulation scheme for indoor visible light communications," in *2017 IEEE/CIC International Conference on Communications in China (ICCC)*, Oct 2017, pp. 1–5.

[14] H. S. Hussein and M. Hagag, "Optical mimo-ofdm with fully generalized index-spatial led modulation," *IEEE Communications Letters*, vol. 23, no. 9, pp. 1556–1559, Sep. 2019.

[15] T. Datta, H. S. Eshwaraiah, and A. Chockalingam, "Generalized space-and-frequency index modulation," *IEEE Transactions on Vehicular Technology*, vol. 65, no. 7, pp. 4911–4924, July 2016.

[16] Xiang-chuan Gao, Jian-kang Zhang, and J. Jin, "Linear space codes for indoor mimo visible light communications with ml detection," in *2015 10th International Conference on Communications and Networking in China (ChinaCom)*, Aug 2015, pp. 142–147.

[17] M. Biagi, A. M. Vegni, S. Pergoloni, P. M. Butala, and T. D. C. Little, "Trace-orthogonal ppm-space time block coding under rate constraints for visible light communication," *Journal of Lightwave Technology*, vol. 33, no. 2, pp. 481–494, Jan 2015.

[18] Z. Ghassemlooy, W. Popoola, and S. Rajbhandari, *Optical Wireless Communications: System and Channel Modelling with MATLAB®, Second Edition*. CRC Press, 05 2019.

[19] T. Komine and M. Nakagawa, "Fundamental Analysis for Visible-Light Communication System Using LED Lights," *IEEE Trans. Consum. Electron.*, vol. 50, no. 1, pp. 100–107, Feb. 2004.